



## Performance Study of E-Nose Measurement Chamber for Environmental Odour Monitoring

Giacomo Viccione<sup>\*a</sup>, Tiziano Zarra<sup>b</sup>, Stefano Giuliani<sup>b</sup>, Vincenzo Naddeo<sup>b</sup>,  
Vincenzo Belgiorno<sup>b</sup>

<sup>a</sup> LIDAM, University of Salerno, via Ponte don Melillo, 1, 84084 Fisciano (SA), Italy

<sup>b</sup> SEED, University of Salerno, via Ponte don Melillo, 1, 84084 Fisciano (SA), Italy  
([gviccion@unisa.it](mailto:gviccion@unisa.it))

Offensive odours from industrial and sanitary environmental engineering plants can cause problems, such as sleep disorders, migraine and loss of appetite, also considering that they address the quality of life.

Odour emission characterization is currently discussed in international literature as to determine its most feasible implementation. A method for continuous odour monitoring is based on the use of electronic noses.

Electronic nose is an instrument which comprises an array of electronic chemical sensors with partial specificity and an appropriate pattern recognition system, capable of recognizing simple or complex odours.

Aim of this work is to numerically analyze the performance of a sensor chamber in order to improve sensor response signals in terms of stability, reproducibility and response time. Comparative results are based on the location of four different diffusers. The numerical analysis was performed by a computational fluid dynamic (CFD) software in order to guarantee that all sensors are exposed to the same chemical sample under the same experimental conditions for the same time, reducing the presence of stagnant or recirculating regions.

### 1. Introduction

In communities exposed to odorous emissions, even though there may be no immediately apparent diseases or infirmities, it is clear that physical, as well as mental, wellness is not promoted (Zarra et al., 2008; Zarra et al., 2009; Zarra et al., 2010).

The environmental monitoring is a very promising field of applications for the electronic nose (Bourgeois et al., 2003).

Electronic nose is an instrument which comprises an array of electronic chemical sensors with partial specificity and an appropriate pattern recognition system, capable of recognizing simple or complex odours (Gardner et al., 1994). In environmental systems, an electronic nose uses an array of sensors with partial overlapping sensitivities to classify and recognise odours (Gardner et al., 1994). Generally, it is composed of a sampling system, a sensor array, a data acquisition system and a pattern recognition algorithm. The role of the sampling system is to collect and convey the volatile sample to the sensors, then to restore previous conditions by means of a cleaning procedure. The interaction between sensors and odours is the first fundamental step of the data acquisition process, since its execution influences all successive steps.

Several papers have been published describing methods to improve or optimise performances of e-nose systems (Gardner et al, 1994; Mielle et al., 2000; Sironi et al., 2007), but a few contributions are reported in literature on sensor chamber used in electronic noses which also plays an important role in the sampling process (Lezzi et al., 2001).

The key point into designing the related geometry is to assure that the injected volatile sample reaches steady and uniform conditions within the chamber in a time period as low as possible, minimizing the presence of stagnant and/or recirculating regions and, therefore, maximizing the contact surface with sensors. For instance, in Scott et al. (2004), it has been found that sensors position strongly affect their response.

In order to accomplish the previous mentioned conditions, a diffuser may be therefore placed inside the chamber, as will be specified later on.

The work presents a fluid dynamic study of sensor chamber in order to guarantee homogeneous flow conditions, low velocity gradients and stagnant volumes. A fully 3D computational fluid dynamic (CFD) study of a special designed sensor chamber, aimed to optimizing the performance, is discussed. The employed code solves the Navier–Stokes equations for compressible fluid moving inside a complex geometry domain. Optimum conditions were found and discussed.

## 2. Materials and methods

### 2.1 Sensor chamber description

The sensor chamber consists of a cylindrical small hollow body with 16 small detectors set over two different horizontal layers (8 for each level, positioned in a polar pattern). An internal cylindrical diffuser is placed in the lower central zone of the chamber, as shown in Figure 1.

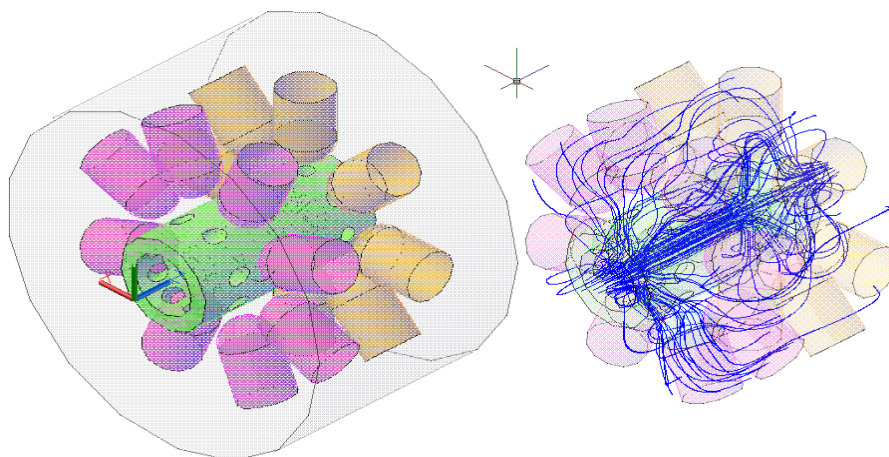


*Figure 1: Isometric view of the sensor chamber: (left), inner space comprises: a central diffuser (green coloured) and 16 sensors (magenta and orange coloured, respectively for the lower and upper layer). (right) volatile sample streamlines surrounding sensors at time  $t = 50$ secs.*

The diffuser is fed through a circular orifice where the volatile sample is injected in, by means of an external pump with point of aspiration placed to the opposite upper side. Four different kind of diffusers (D1-D4) were considered, as shown in Figure 2. They basically differ in the spatial allocation of the inner pipelines.

The purpose is the same: to scatter the injected volatile compound in a way it reaches an homogeneous state near the detectors, with low spatial speed variation. In addition, stagnant and recirculating regions have to be attenuated. This aspect is crucial since it should be ensured that all sensors are in contact with the same volatile fraction, for the same time period.

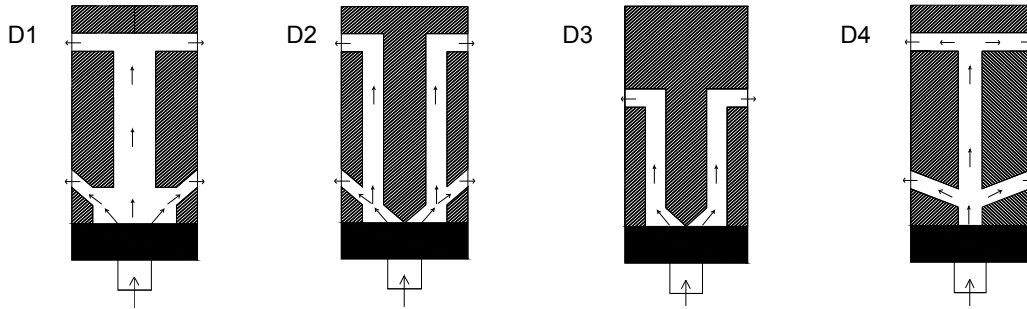


Figure 2: Vertical cross section of the four diffusers (D1 - D4) considered in the CFD analysis.

The presence of a diffuser, such as the one above described, is therefore needed. It is indeed proved that without its allocation, the injected volatile sample only takes the central portion of the chamber, leaving the detectors nearly untouched. The main drawback related to both the inlet and outlet hole diameter  $d_h$ , compared to the crosswise chamber size  $d_c$  is overcome. The ratio  $d_h/d_c$ , being much less than unity, would imply the flow with a predominant direction – the space between holes – with most of the inner space occupied by stagnant or recirculating zones.

As can be seen later in the paper, spatial gas mixture distribution inside the chamber is strongly affected by channels' allocation inside the diffuser. The optimal one will be chosen on the basis of two factors: the time needed to reach steady conditions of motion – which has to be minimized – and the volatile fraction, which need to be as constant as possible.

## 2.2 CFD analysis

Four different internal diffusers are taken into account. The best is chosen comparing numerical results of computations carried out using Flow 3D<sup>®</sup> (Flow Sciences User Manual, 2009). It is based on the numerical solution of the Navier Stokes equations in a Eulerian framework:

$$\frac{\partial \rho}{\partial t} + \text{div } \rho \mathbf{v} = 0 \quad (1)$$

$$\left( \frac{\partial \mathbf{v}}{\partial t} + \mathbf{v} \cdot \nabla \mathbf{v} \right) \rho = \nabla p + \nabla \cdot \mathbf{T} + \mathbf{f} \quad (2)$$

where  $\mathbf{v}$  is the flow velocity,  $\rho$  is the fluid density,  $p$  is the pressure,  $\mathbf{T}$  is the (deviatoric) stress tensor, and  $\mathbf{f}$  represents body forces (per unit volume) acting on the fluid. The first equation states the conservation of mass within a unit volume whereas the second states the conservation of momentum, that is an application of the Newton's second law to a continuum. The equations are closed including the k-eps turbulence model. It has been shown to provide reasonable approximations to many types of flows. In the cases here presented, once a nearly steady state is attained, high Reynolds numbers are reached, and natural instabilities that occur within gases are not damped out and they manifest in the creation of eddies of various length scales.

The injected volatile sample has the following physical properties:

- density ( $\rho$ ) = 1.2 kg/m<sup>3</sup>
- dynamic molecular viscosity ( $\mu$ ) = 1.8 10<sup>-5</sup> kg / ms.

As boundary conditions, a constant volume discharge of 300 mL/min is injected from the bottom hole. The outflow condition on the upper hole is imposed instead. As a result, once reached the final steady state, about the same discharge is ejected. Inner space is initially filled with standard atmosphere having pressure equal to 101,330 Pa. Time calculation is 100 s for all simulations. Time step size is automatically updated and controlled by stability and convergence criteria. Minimum time step size has been equal to 5·10<sup>-3</sup> s.

Such a software is well suited for the present investigation, because it allows the simulation of two gases (multifluid simulation) moving in complex 3D geometries. It basically provides two methods to

track fluid interfaces: the sharp and diffuse interface algorithms. Each of them is best suited for a certain type of flow problem. Here, the sharp interface method is chosen, in order to clearly track its position in time. A special Volume of Fluid (VOF) advection method (Hirt and Nichols, 1981) based on a 3D reconstruction of the gas interface has been developed and implemented in Flow 3D. The interface is reconstructed in 3D using a piecewise linear representation, where the interface is assumed to be planar in each control volume (or cell) containing the interface.

The relative motion is assumed for simplicity under isothermal condition (gases at constant temperature, being equal to 293.15K, with no heat transfer).

The chamber is previously built by means of 3D objects assembled in a CAD software and then exported as stl file in order to be implemented inside Flow 3D geometry environment. A Cartesian coordinate system (x, y, z) was adopted with the Z axis placed along the flow direction inside holes and the XY plane coinciding with sensors layers. In particular, a computational 3D grid is placed over the simulating space, employing 60 cells x 60 cells along the horizontal plane and 45 cells along the vertical direction. Cell size is therefore equal to 2 mm. In addition, in order to check such a spatial discretization in terms of attained results, a single simulation with a unit cell of 1x1x1 mm has been executed. Volatile distribution around the chamber does not change accordingly, reaching the conclusion that the employed spatial discretization is proper.

### 3. Results

Depending on the specific diffuser adopted, different times ( $t_f$ ) to reach a nearly stationary motion are needed as specified in Table 1. The steady state is an asymptotic condition (it is reached after an indefinite time), hence the nearly steady state is reached when the percentage of temporal variation of hydrodynamic variables is lower than  $10^{-4}$  near the sensors.

*Table 1: Times  $t_f$  needed to reach stationary motion, as function of the diffuser.*

Diffuser type	$t_f$ (s)
D1	60
D2	85
D3	90
D4	58

Results highlight that diffuser D4 yields the lower transitory period after which the involved hydrodynamic variables exhibit a temporal variation negligible, as specified above. Maximum velocity magnitude and spatial velocity gradients near the sensors are below 1cm/s and  $10^{-4}$ cm/s<sup>2</sup> respectively. All the simulations reached the nearly steady state after 90 s (worst condition shown in Table 1 for diffuser D3).

Figure 3 shows the comparison of volume percentage (V1) trends for the injected volatile sample as function of the diffuser adopted. It is defined as the ratio between the amount of the injected volume inside the chamber over the total inner volume available.

Stagnant and recirculating region locations are also affected by the particular diffuser employed. The complementary final volume percentage ( $V_{f,2}$ ), related to recirculating and stagnant regions in the chamber at time  $t_f$ , is specified in the Table 2.

*Table 2: Complementary final volume percentage  $V_{f,2}$  taken by the gas already present in the chamber, as function of the adopted diffuser.*

Diffuser type	$V_{f,2}$ (%)
D1	16
D2	27
D3	35
D4	11

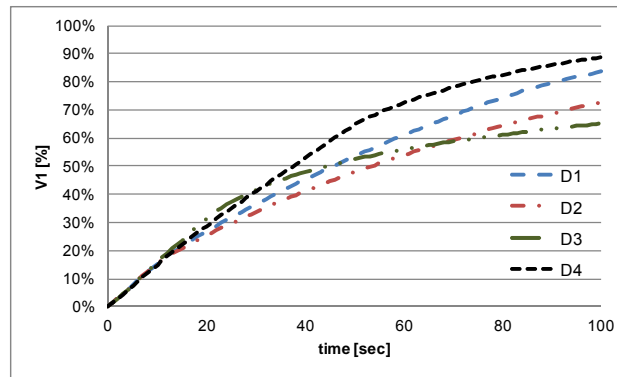


Figure 3: Volume percentage (referred to the inner volume available) versus time, of the injected volatile sample ( $V_1$ )

The presence of a single layer of pipelines in diffuser D3 yields worst results: about a third of the available volume is still taken by the gas previously inside the chamber. Best performance is instead shown by diffuser D4. Vertical cross sections displaying volume distributions are shown in Figure 4.

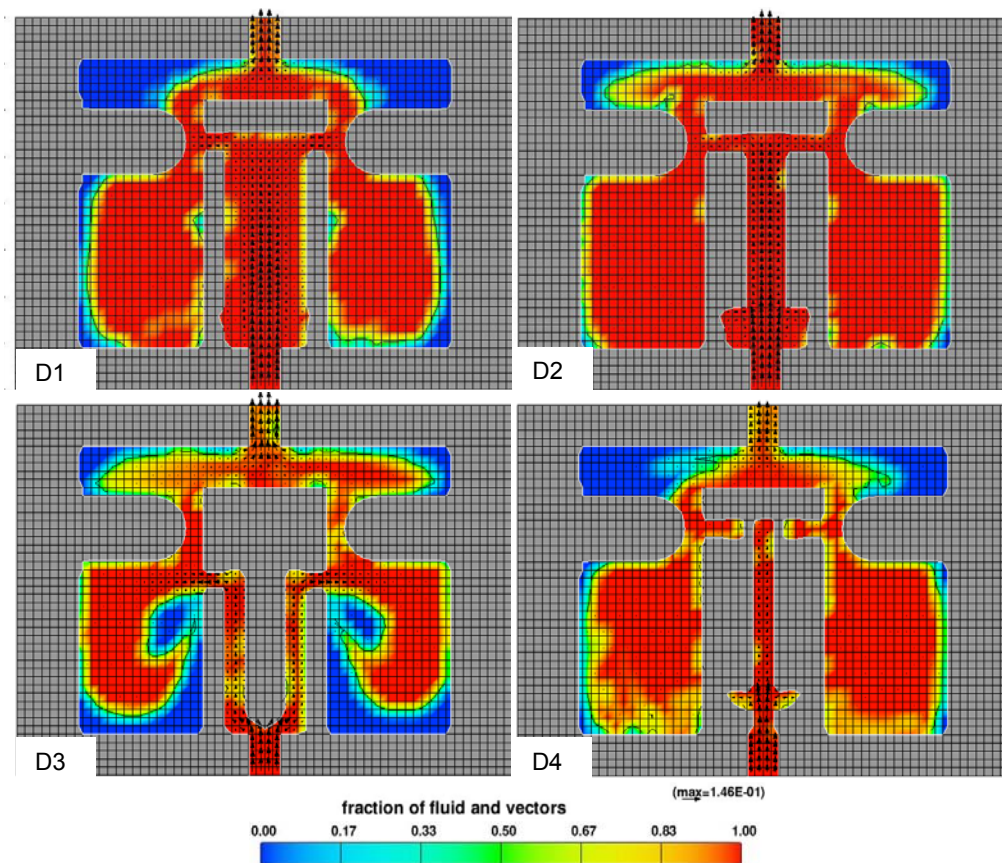


Figure 4: Displacement of gases inside the chamber at times  $t_f$  (see Table 1). Contour plot refers to the volume fraction of injected volatile sample (gas 1). Velocity vectors are scaled in terms of the maximum magnitude (m/s) on the arrow.

The results confirm that the best performance of the e-nose chamber are obtained through the use of the diffuser D4. The advantage into using such a diffuser is twofold: the time  $t_f$  needed to reach nearly steady condition and the amount  $V_{f,2}$  of recirculating and stagnant regions are the smallest values respectively in Table 1 and Table 2.

#### 4. Conclusions

The fluid dynamic study of a cylindrical sensor chamber was carried out to assess performances of electronic nose in order to improve the sensor chamber design. This study was performed by creating a 3D model of the sensor chamber, discretizing the computational domain in finite volumes and numerically solving the transport equations of both momentum and mass (Navier-Stokes equations). Four types of diffuser have been taken into account. The best is provided by the minimum of two variables: the time  $t_f$  (Table 1) and the volume percentage  $V_{f,2}$  (Table 2).

Numerical simulations showed the need of a diffuser in sensor chamber in order to minimizing the presence of stagnant and/or recirculating regions and, therefore, maximizing the contact surface with sensors.

#### References

- Bourgeois W., Romain A.C., Nicolas J., Stuetz R.M., 2003. The use of sensor arrays for environmental monitoring: interests and limitations, *J. Environ. Monit.* 5, 852–860.
- Flow Sciences 2009.Inc. Flow-3D User Manual, release 9.4 , Santa Fe, NM, USA
- Gardner J.W., Bartlett P.N., 1994. A brief history of electronic noses. *Sens. Actuators B*, 18–19, pp. 211–220.
- Hirt C.W., Nichols, B.D., 1981, Volume of Fluid (VOF) Method for the Dynamics of Free Boundaries. *Journal of Computational Physics* 39, 201–225.
- Lezzi A.M., Beretta G.P., Comini E., Faglia G., Galli G., Sberveglieri G., 2001. Influence of gaseous species transport on the response of solid state gas sensors within enclosures, *Sens. Actuators B* 78, 144–150.
- Mielle P., Marquis F., Latrasse C., 2000. Electronic noses: specify or disappear, *Sens. Actuators B* 69, 287–294.
- Scott S.M., James D., Ali Z., O'Hare W.T., 2004, *Journal of Thermal Analysis and Calorimetry*, 76, 693-708.
- Zarra T., Naddeo V., Belgiorno V., Reiser M. and Kranert M., 2008. Odour monitoring of small wastewater treatment plant located in sensitive environment. *Water Sci. Technol.* 58 (1), pp. 89-94.
- Zarra T., Naddeo V., Belgiorno V., Reiser M., Kranert M., 2009. Instrumental characterization of odour: a combination of olfactory and analytical methods. *Water Science and Technology*, Vol. 59 (8), 1603-1609.
- Zarra T., Naddeo V., Giuliani S., Belgiorno V., 2010. Optimization of field inspection method for odour impact assessment. *Chemical Engineering Transactions*, 23, 93-98.